ACS OMEGA

http://pubs.acs.org/journal/acsodf

Article

Conductive Aramid Fibers from Electroless Silver Plating of Crosslinked HPAMAM-Modified PPTA: Preparation and Properties

Xue Geng, Xiangyu Kong, Shengnan Geng, Rongjun Qu,* Jiafei Wang, Ying Zhang, Changmei Sun,* and Chunnuan Ji

Cite This: *ACS Omega* 2022, 7, 17014−17023

Read Online

ACCESS | Metrics & More | Article Recommendations

ABSTRACT: Conductive aramid (PPTA) fibers are highly needed for making flexible conductive materials, antistatic materials, and electromagnetic shielding materials. In this work, silver-plated conductive PPTA fibers with high conductivity and excellent mechanical properties were prepared by the electroless plating of PPTA fibers modified with crosslinked hyperbranched polyamide-amine (HPAMAM). The crosslinked HPAMAM creates a stable interface between the PPTA fibers and the silver plating. The morphology and physicochemical properties of the modified and the silver-plated fibers were characterized by Fourier transform infrared spectroscopy, scanning electron microscopy, atomic force microscopy, X-ray diffraction, X-ray photoelectron spectroscopy, and thermogravimetric analysis. Three epoxy crosslinking agents with different chain lengths were used to crosslink HPAMAM, and the effects of HPAMAM concentration, crosslinking agent dosage, and crosslinking time on the resistance of the fibers were studied. The long chain crosslinking agent appears to be beneficial to silver plating. The lowest resistance (0.067 Ω/cm) was attained when HPAMAM was modified by diethylene glycol diglycidyl ether (1:1 molar ratio), and 20 g/L HPAMAM was used to modify the PPTA fibers. The tensile strength of the original PPTA fibers decreased by only 3% or less after silver plating.

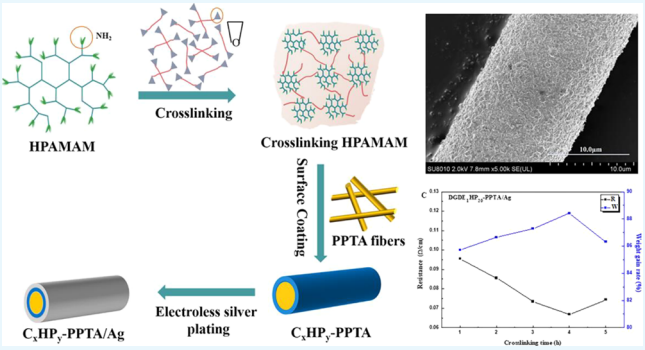

1. INTRODUCTION

Para aramid fibers, that is, poly(*p*-phenylene terephthamide) fibers, are well known for their high strength, high modulus, and high crystallinity.[1−3] They have not only excellent mechanical properties but also outstanding thermal stability, chemical stability, heat resistance, and flame retardant ability. Para aramid fibers (commonly referred to as PPTA fibers) were first produced in 1972 and have since then been widely used in diverse areas such as military applications, aerospace industry, electrical engineering, and so on.[2,4,5] Because PPTA fibers are excellent materials for electrical insulation, they can easily generate and accumulate substantial static electricity that can damage electronic equipment and textiles during their use.[6] Static electricity can also be a fire hazard and negatively impact human health.[7−9] The electromagnetic interference from PPTA fibers can also interrupt the normal functioning of electronic devices,[10] and cancer risk escalates when people are exposed to prolonged electromagnetic radiation. As a result, there is a considerable demand for specialized aramid fibers that are free from the problems due to static electricity and electromagnetic interference.

Conductive aramid fibers have attracted extensive attention from researchers, as they can be used to fabricate functional fiber devices.[11,12] Various methods have been reported to prepare conductive aramid fibers, for example, blend spinning of conductive components and aramid polymers,[13] chemical coating with conductive polymers,[14] electrodeposition and electroless deposition of silver, nickel, or other metals,[15,16] and vacuum or sputter plating.[17] Electroless plating is advantageous, in that it does not need large-scale instruments and equipment, which makes it possible to fabricate conductive aramid fibers at industrial scale.[18−20] In addition, the electroless plating process does not damage the mechanical properties of the fibers, which is essential in ensuring the usability of the fiber products.

Because the surface of PPTA fibers is smooth, has low roughness, and lacks active sites for the deposition of metal particles, PPTA fibers need to be modified effectively before electroless plating.[21,22] Liang et al.[23] roughened aramid fibers

Received: January 8, 2022
Accepted: February 18, 2022
Published: May 9, 2022

https://doi.org/10.1021/acsomega.2c00143
ACS Omega 2022, 7, 17014−17023

Table 1. Formulation for Modifying PPTA with Crosslinked HPAMAM

	HPAMAM			dosage of crosslinking agent (mL)		
product	concentration (g/L)	mass (g)	molar ratio to crosslinking agent[a]	ECH	EGDE	DGDE
C_1HP_{10}-PPTA	10	0.50	1:1	0.060	0.105	0.125
C_1HP_{15}-PPTA	15	0.75		0.090	0.158	0.188
C_1HP_{20}-PPTA	20	1.00		0.120	0.210	0.250
C_1HP_{25}-PPTA	25	1.25		0.150	0.263	0.313
C_1HP_{30}-PPTA	30	1.50		0.180	0.315	0.375
C_2HP_{20}-PPTA	20	1.00	1:2	0.240	0.420	0.500
C_3HP_{20}-PPTA			1:3	0.360	0.630	0.750
C_4HP_{20}-PPTA			1:4	0.480	0.840	1.000
C_5HP_{20}-PPTA			1:5	0.600	1.050	1.250

[a]Calculated by taking the average molecular weight of HPAMAM as 750.

with a self-made metallization reagent (NaH-DMSO) and prepared silver-plated conductive aramid fibers by electroless plating. However, the coarsening process destroys the skin structure of the fibers and thus decreases the breaking strength of the fibers (6.5%). Wang et al.[24] constructed an organic polymer transition layer to avoid the direct contact of aramid fibers and the metal coating. Specifically, polydopamine is used to treat meta-aramid fibers, and electroless plating is accomplished with silver that is autocatalytic adsorbed on the surface of polydopamine. However, the high price of dopamine precludes the use of this method at a larger scale.

Hyperbranched polyamide-amine (HPAMAM) dendrimers are a type of polyamide-amine dendrimers.[25,26] The outside of these three-dimensional and highly branched dendrimers is covered by many N and O functional groups, and the inside has substantial cavities.[27,28] They can thus be used as a high-capacity chelating agent and catalyst carrier for metal ions, and they play a crucial role in various areas including adsorption, catalysis, drug delivery, and so on.[29−31] Whereas other dendritic polyamide-amine dendrimers have very symmetrical and regular structures that require delicate step-by-step synthesis through costly and tedious protection, separation, and purification steps, HPAMAM has an irregular ellipsoid shape that allows a simple, economical, one-pot synthesis, and yet, it still retains very similar material properties.[32] Therefore, HPAMAM is more suitable for large-scale industrial applications.[33] Coating HPAMAM dendrimers on the surface of the fibers can increase the roughness and improve the surface activity of the fibers. More importantly, the coated HPAMAM dendrimer layer can act as a secondary reaction platform to bind metal ions and then reduce in situ to form metal nanoparticles as catalytic activation centers in electroless plating, which helps to avoid the complicated and costly pretreatment process in traditional electroless plating that requires individual coarsening, sensitization, and activation steps.[34]

In this work, we prepared a series of conductive PPTA fibers by the electroless silver plating of Kevlar 49 PPTA fibers that are modified with crosslinked HPAMAM. The crosslinked HPAMAM improves the surface activity and roughness of the PPTA fibers and provides a reaction platform for the subsequent silver plating that relies on the chelation of Ag(I) by HPAMAM. We systematically investigated the factors that influence the electrical conductivity and the mechanical properties of the conductive fiber, including the type and dosage of crosslinking agent, the reaction time of crosslinking, and the dosage of HPAMAM.

2. EXPERIMENTAL SECTION

2.1. Materials. All chemicals were used as received unless stated otherwise. PPTA fibers (Kevlar 491420D) were purchased from DuPont, Inc. (USA). HPAMAM was purchased from Weihai CY Dendrimer Technology Co., Ltd. (China). Epichlorohydrin (ECH), methyl alcohol, glucose, and silver nitrate ($AgNO_3$) were purchased from Sinopharm Chemical Reagent Co., Ltd. (China). Ethylene glycol diglycidyl ether (EGDE) and polyvinylpyrrolidone (PVP) were purchased from Shanghai Macklin Biochemical Co., Ltd. (China). Industrial grade diethylene glycol diglycidyl ether (DGDE) was purchased from Anhui Xinyuan Technology Co., Ltd. (China). Polyethylene glycol 2000 (PEG) was purchased from Tianjin BASF Chemical Trade Co., Ltd. (China). All chemicals except DGDE were analytical grade.

2.2. Preparation of Silver-Plated PPTA Fibers. A specified amount of HPAMAM in methanol (100 mL) was magnetically stirred for 30 min at 60 °C to form a solution (10−30 g/L HPAMAM in MeOH) before the addition of the crosslinking agent (ECH, EGDE, or DGDE; stoichiometry of the HPAMAM/crosslinking agent varies from 1:1 to 1:5; see Table 1). The mixture was maintained at 60 °C under magnetic stirring for 5 h to give the crosslinked HPAMAM that is introduced onto the PPTA fibers (see below). The obtained crosslinked HPAMAM gels are referred to as C_xHP_y, where C is the crosslinking agent (or the group in aggregate), x indicates the molar ratio of HPAMAM to the crosslinking agent, and y indicates the amount of HPAMAM used in the synthesis.

The commercial PPTA fibers were cleaned in a Soxhlet extractor first with acetone at reflux for 24 h and then with ethanol at reflux for 24 h. The cleaned fibers were dried in a vacuum oven at 60 °C to constant weight.[35] The dried PPTA fibers were soaked in the solution of the crosslinked HPAMAM at room temperature for 60 min and then cured at 60 °C to constant weight. The obtained fibers were denoted as C_xHP_y-PPTA, where C is the individual crosslinking agent (or the group in aggregate), *x* indicates the molar ratio of HPAMAM to the crosslinking agent, and *y* indicates the amount of HPAMAM loaded onto the fibers. The fibers treated with the ECH-crosslinked HPAMAM was washed with 0.1% aqueous Na_2CO_3 after curing to remove the HCl generated in the crosslinking reaction, then washed with deionized water, and dried at 60 °C to constant weight.

The silver plating bath was prepared based on a published procedure.[36] To an aqueous solution of silver nitrate (25 g/L, 100 mL) was added dropwise ammonium hydroxide until the

https://doi.org/10.1021/acsomega.2c00143
ACS Omega 2022, 7, 17014−17023

Scheme 1. Fabrication of CxHPy-PPTA/Ag

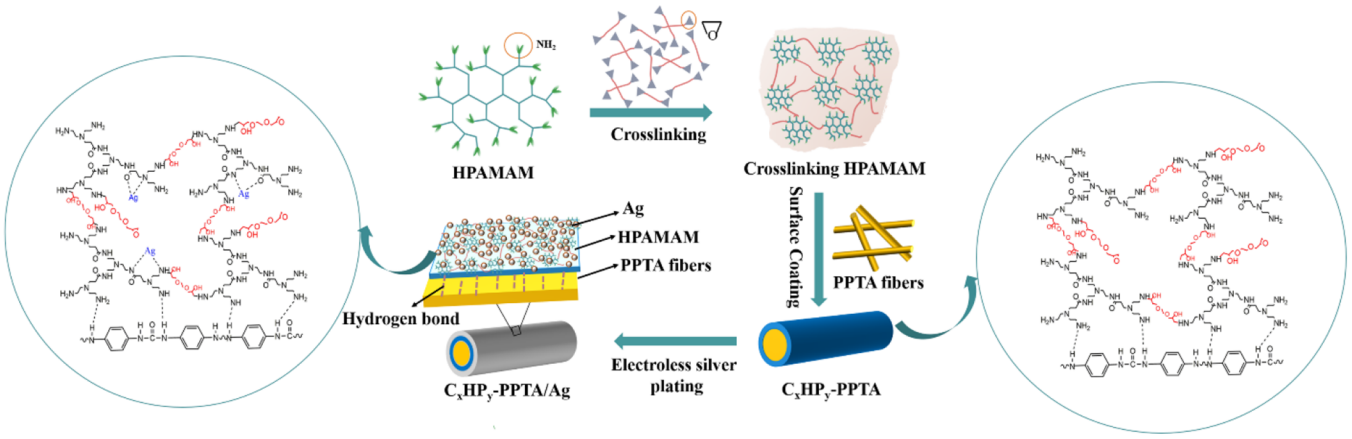

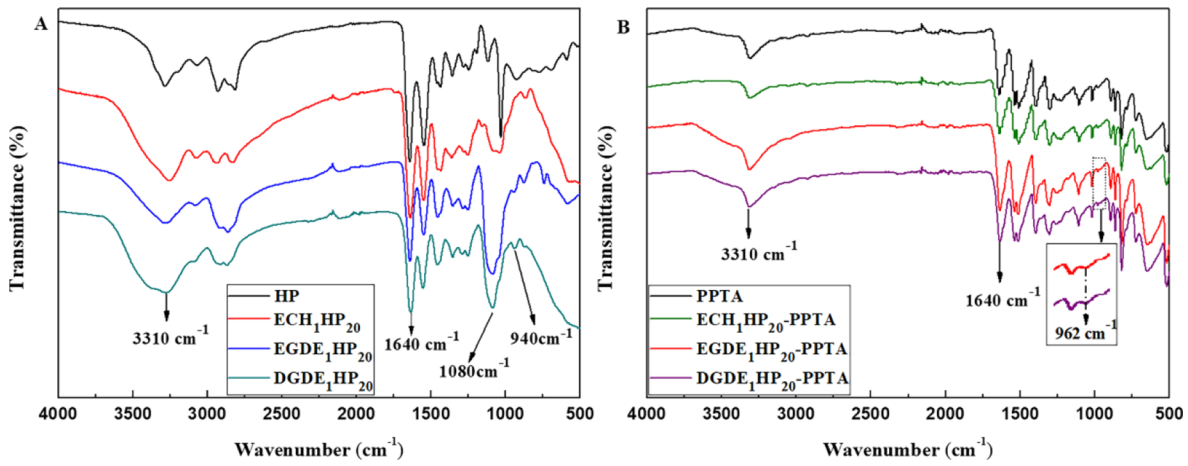

Figure 1. IR spectra of crosslinked HPAMAM gels (A) and crosslinked HPAMAM-modified PPTA fibers (B).

solution became clear and transparent. The solution pH was then adjusted to 11.0 by slow dropwise addition of aqueous KOH (6 g/L), and ammonium hydroxide was added dropwise again until the solution clarified. Finally, PVP (0.5 wt %) was added to this mixture to give the silver plating bath. Meanwhile, a reduction solution consisting of glucose (of 30 g/L), PEG (stabilizer, 75 mg/L), and anhydrous ethanol (dispersant, 40 mL/L) in water was prepared.

To carry out the electroless silver plating, C_xHP_y-PPTA (0.5 g) was immersed in the abovementioned plating bath for 30 min at room temperature with ultrasonication, and then the reduction solution (100 mL) was added slowly (about 1 drop per second) at 30 °C. After the addition was complete, the mixture was maintained at 30 °C under ultrasonication for 60 min. The fibers were collected by filtration, washed with deionized water for three times, and then dried in an oven at 60 °C to constant weight. The obtained silver-plated aramid fibers are denoted as C_xHP_y-PPTA/Ag.

To test the firmness of binding for the C_xHP_y-PPTA/Ag fibers,[24] the fibers were washed ultrasonically (40 kHz) with distilled water at 30 °C for 10 min and dried in a vacuum oven at 60 °C to constant weight before characterization. The washing/drying procedure was repeated for five cycles.

2.3. Characterizations. Infrared spectra of the modified fibers and the crosslinked HPAMAM gels were measured on a Nicolet iS50 Fourier transform infrared (FTIR) spectrophotometer (Nicolet, USA) over 500−4000 cm^{-1}. The surface morphologies of the PPTA fibers were investigated using a SU8010 field emission scanning electron microscope (Hitachi, Japan) at 25.0 kV accelerating voltage. X-ray photoelectron spectroscopy (XPS) was carried out on an ESCALAB Xi^+ instrument (Thermo Fisher Scientific, USA) in the CAE mode at 30.0 eV pass energy. The crystalline structure of the samples was analyzed on a D-MAX 2200VPCX X-ray diffractometer (Rigaku, Japan) using Cu Kα radiation at a scan rate of 15°/min, and the diffraction patterns were recorded in the reflection mode over 2θ = 5° − 90°. The thermal decomposition curves of the fibers were recorded on a TG/DSC synchronous thermal analyzer (STA 409 PC/PG, NETZSCH, Germany) over 30−800 °C under a nitrogen atmosphere at a heating rate of 10 °C/min. The weight gain rate was determined using an analytical balance to measure the mass of the fibers before and after silver plating.

At least 20 specimens were prepared for each test of tensile strength or electrical resistance. The tensile strength of the fibers was tested on a single fiber electronic strength meter (YG001B, Taicang Hongda, China) at 10 mm/min tensile speed and 30 mm gauge length. The electrical resistance of the silver-plated PPTA fibers (5 cm sample length) was measured using a Fluke 8846A (USA) multimeter at room temperature.

3. RESULTS AND DISCUSSION

Scheme 1 illustrates the processes of crosslinking, modification, and silver plating. In crosslinking, the epoxy groups of the

https://doi.org/10.1021/acsomega.2c00143
ACS Omega 2022, 7, 17014−17023

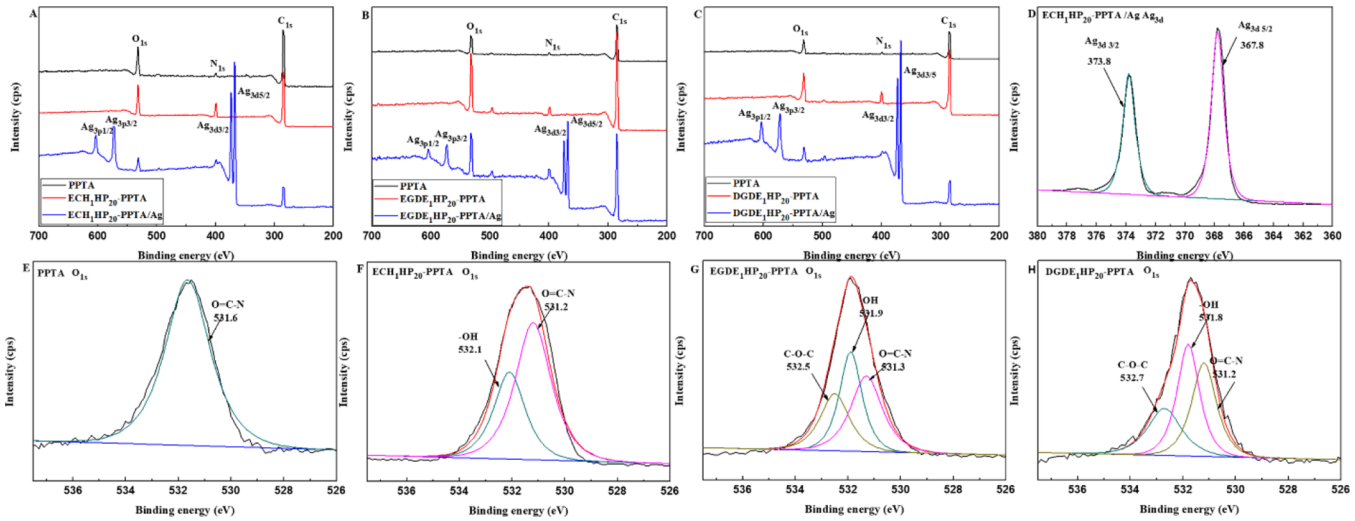

Figure 2. Wide scan XPS spectra of C_1HP_{20}-PPTA samples and C_1HP_{20}-PPTA/Ag samples (A–C) and high-resolution XPS spectra of Ag_{3d} (D) and O_{1s} (E–H).

Table 2. Element Content and Crystalline Parameters of Pristine and Modified PPTA

	ratio of element concentrations		2θ (°)		FWHM (°)		Lhkl (nm)		
samples	N/C	O/C	(110)	(200)	(110)	(200)	(110)	(200)	CI (%)
PPTA	0.058	0.215	20.56	22.90	1.32	1.75	4.32	3.88	75.52
ECH_1HP_{20}-PPTA	0.161	0.223	20.55	22.89	1.34	1.76	4.32	3.88	75.01
$EGDE_1HP_{20}$-PPTA	0.065	0.247	20.85	23.22	1.82	2.03	4.26	3.83	64.84
$DGDE_1HP_{20}$-PPTA	0.147	0.323	20.33	22.67	1.39	1.71	4.36	3.92	58.73

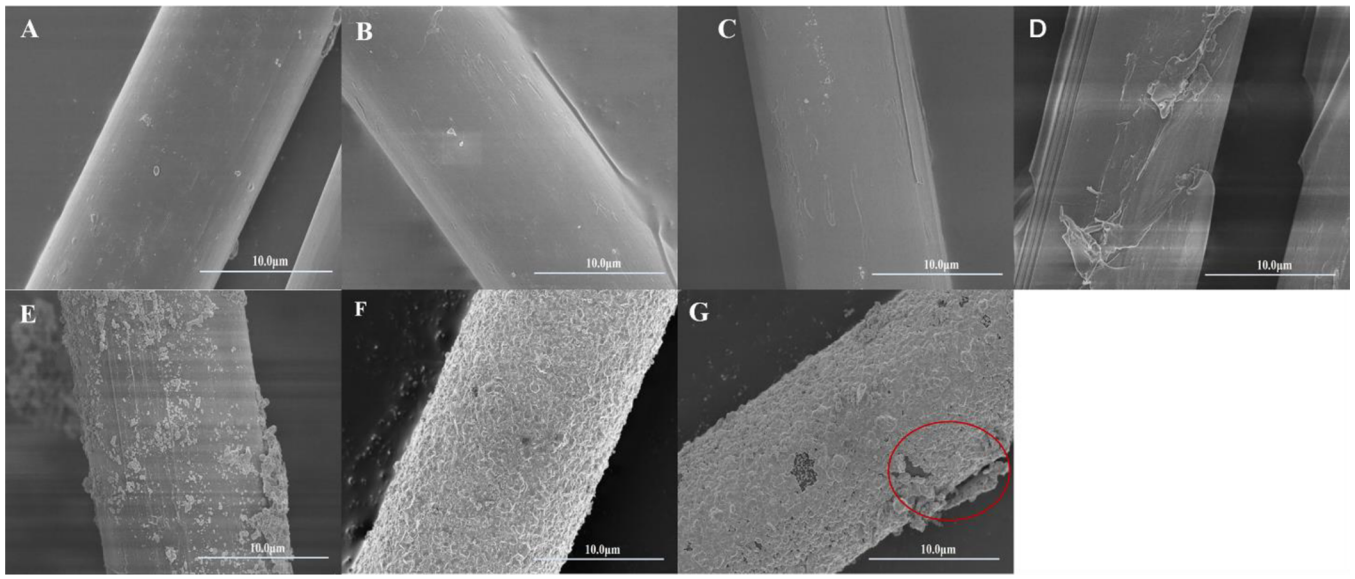

Figure 3. FE-SEM images of PPTA (A), ECH_1HP_{10}-PPTA (B), ECH_1HP_{20}-PPTA (C), ECH_1HP_{30}-PPTA (D), ECH_1HP_{10}-PPTA/Ag (E), ECH_1HP_{20}-PPTA/Ag (F), and ECH_1HP_{30}-PPTA/Ag (G).

crosslinking agent open up and combine with the amino groups of HPAMAM such that multiple HPAMAM molecules become connected to form a network structure. As a coating agent, the crosslinked HPAMAM is then cured on the surface of PPTA fibers through hydrogen bonding during the immersion and drying of the PPTA fibers. Finally, silver particles are deposited on the surface of coated PPTA fibers to form a silver layer through electroless silver plating.

3.1. Characterization of Fibers. The functional groups on the surface of the crosslinked HPAMAM gels and the modified PPTA fibers were analyzed by FTIR spectra with C_1HP_{20} and C_1HP_{20}-PPTA as the representative materials. The absorption peaks around 3284 and 1640 cm^{-1} in the pristine HPAMAM (Figure 1A) correspond to the N–H stretching vibration of the amino group and the C=O stretching vibration of amide group, respectively.[37] Several changes can be noted after crosslinking HPAMAM. First, the absorption

https://doi.org/10.1021/acsomega.2c00143
ACS Omega 2022, 7, 17014–17023

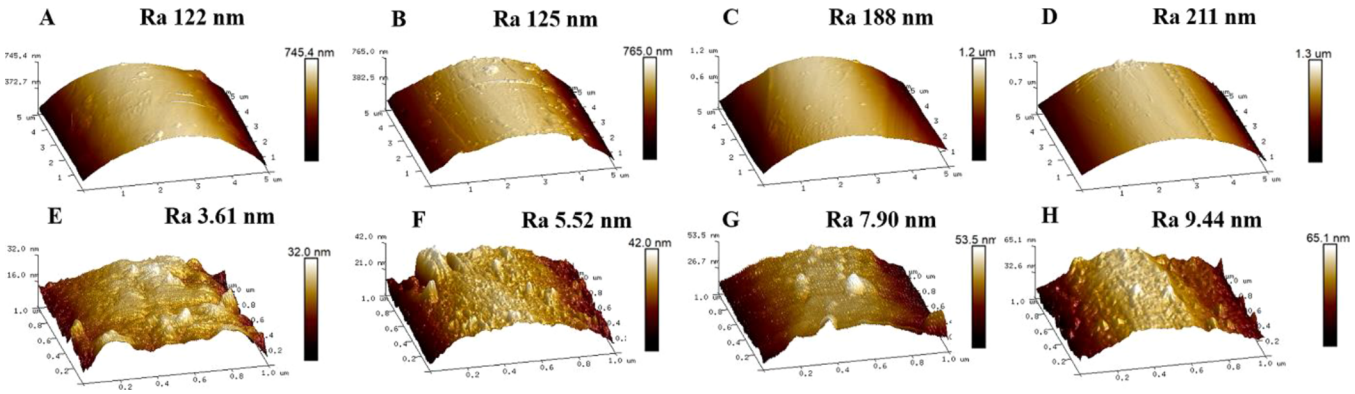

Figure 4. AFM images of PPTA (A, E), ECH_1HP_{10}-PPTA (B, F), ECH_1HP_{20}-PPTA (C, G), and ECH_1HP_{30}-PPTA (D, H).

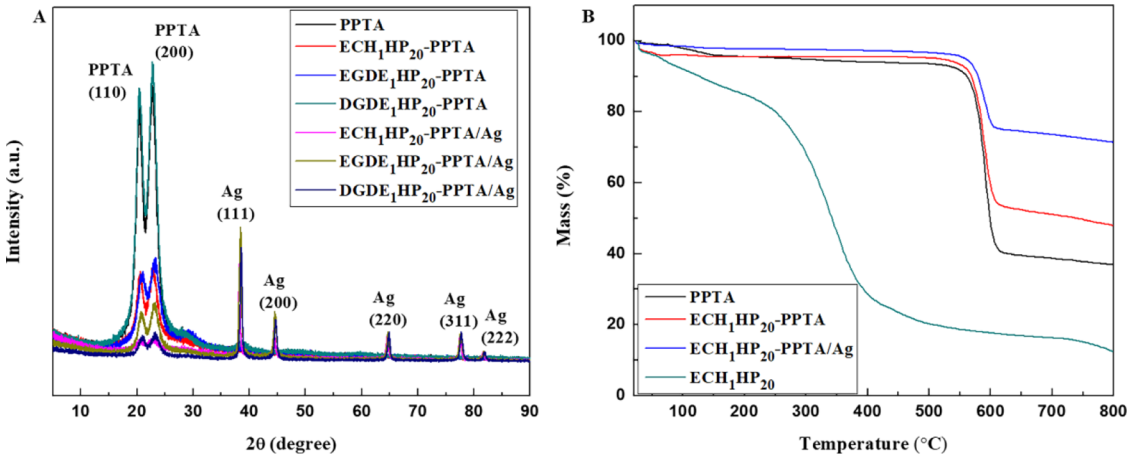

Figure 5. XRD patterns (A) and thermogravimetric diagrams (B) of pristine PPTA fibers, modified fibers, and silver-plated fibers.

peak around 3300 cm^{-1} widens because the stretching vibration peaks of N−H and O−H now overlap. In addition, a wide peak appears at 1080 cm^{-1} due to the overlap of the stretching vibration peaks of C−O and C−O−C.[38] Finally, a new absorption peak appears at 940 cm^{-1} for $EGDE_1HP_{20}$ and $DGDE_1HP_{20}$, which corresponds to the symmetric stretching vibration of the epoxy group.[39] These observations also apply to the modified PPTA fibers (Figure 1B). That is, the HPAMAM has been successfully crosslinked and the PPTA fibers are effectively modified.

The elemental changes on the fiber surface were analyzed by XPS using C_1HP_{20}-PPTA as the representative materials. Compared with the original PPTA, the C_1HP_{20}-PPTA fibers have slightly stronger N_{1s} and O_{1s} peaks (Figure 2). Table 2 shows that the N/C and O/C ratios are higher for the modified fibers. In the high-resolution XPS spectrum of the original PPTA, there is only one O_{1s} peak at 531.6 eV which can be unambiguously attributed to the amide group (O═C−N). In contrast, a new O_{1s} peak at 532.1 eV can be noted in the XPS spectrum of ECH_1HP_{20}-PPTA, which can be attributed to the hydroxyl group that is generated after the ring opening of the epoxy group, and $EGDE_1HP_{20}$-PPTA and $DGDE_1HP_{20}$-PPTA both have three O_{1s} peaks that correspond to O═C−N (531.3 eV), −OH (531.9 eV), and C−O−C (532.5 eV).[40] These observations agree well with the FTIR findings and verify the crosslinking of HPAMAM and the modification of PPTA. The characteristic peaks of $Ag_{3d3/2}$ and $Ag_{3d5/2}$ appear at 373.8 and 367.8 eV after silver plating, which verify the presence of metallic Ag^0.[41]

Figure 3 shows the scanning electron microscopy (SEM) images of the modified and the silver-plated fibers with different formulations. Whereas the original PPTA has a smooth surface, the modified PPTA fibers have a rough surface and are covered with an irregular film. The roughness and the size of the surface particle both increase when the concentration of crosslinked HPAMAM is higher, and serious agglomeration can be noted on the fibers when the HPAMAM concentration is at 30 g/L. The deposition of a silver layer can be clearly seen on the silver-plated fibers. The silver layer is very sparse and discontinuous when the concentration of HPAMAM is low, which implies poor coating, but becomes dense and uniform when the concentration of HPAMAM is 20 g/L. However, when the HPAMAM concentration increases further, part of the silver layer thickens excessively and peels off due to the agglomeration of HPAMAM.

On the atomic force microscopy (AFM) images of the PPTA fibers (Figure 4), the untreated PPTA fibers have a relatively smooth surface and a Ra value of 3.61 nm, whereas the modified PPTA fibers have some particles on the surface and a Ra value that is positively related to the concentration of crosslinked HPAMAM used for coating. The AFM results agree well with the SEM findings.

Figure 5A shows that the original PPTA fibers are partially crystalline with two sharp diffraction peaks in the 2θ range of 15−25°.[1] The surface modification process does not damage the crystal structure of the fibers, as the modified fibers have essentially the same diffraction peaks of the original fibers, although the intensity of the peaks is slightly lower (Table 2),

https://doi.org/10.1021/acsomega.2c00143
ACS Omega 2022, 7, 17014−17023

Table 3. Tensile Strength and Elongation at Break of Different Fibers

		C_1HP_{20}-PPTA			C_1HP_{20}-PPTA/Ag		
	PPTA	ECH	EGDE	DGDE	ECH	EGDE	DGDE
tensile strength (cN/dT)	19.54	18.86	18.85	19.13	18.41	18.02	18.89
elongation at break (%)	2.32	2.21	2.19	2.19	2.11	2.09	2.13

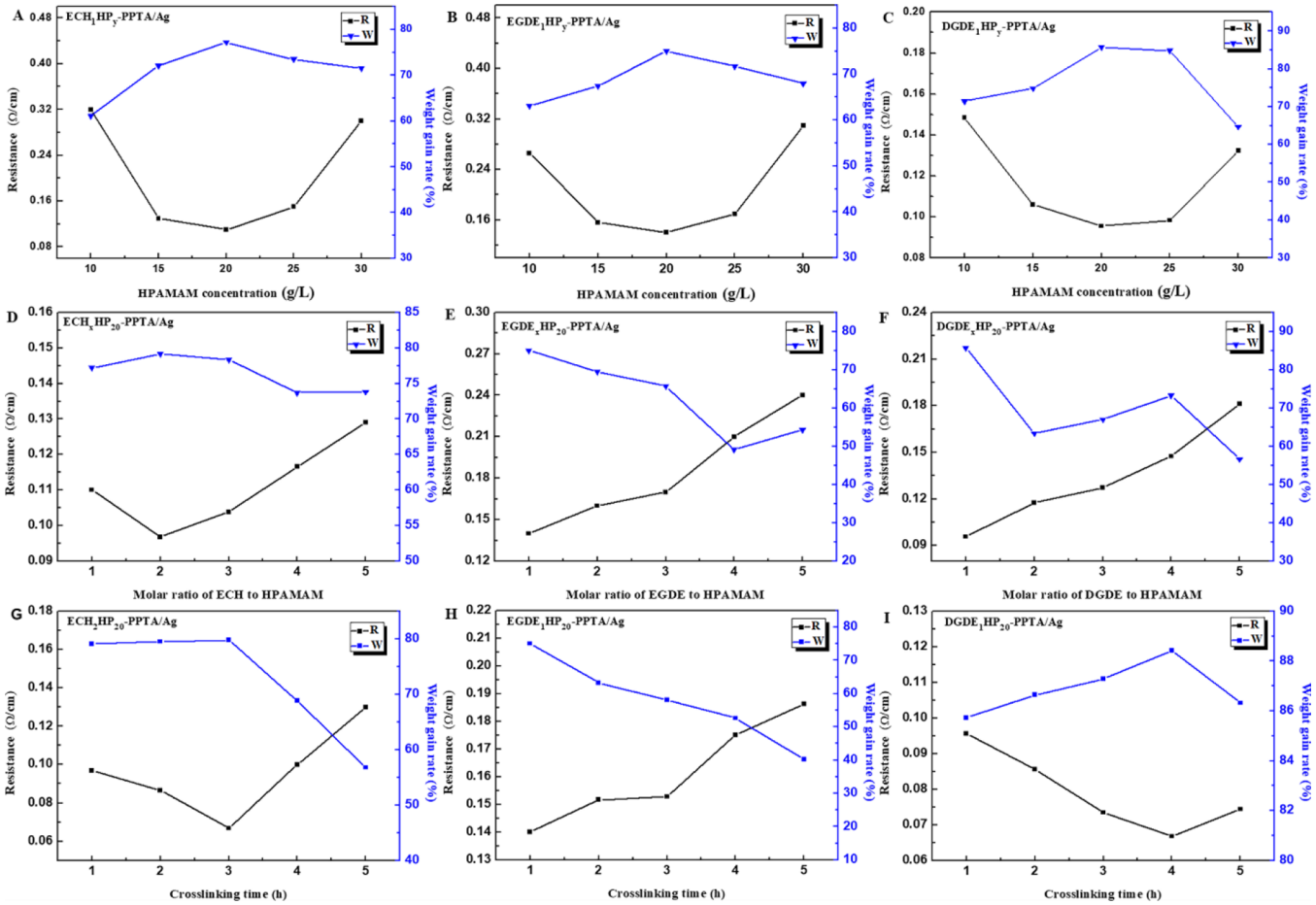

Figure 6. Effect of HPAMAM concentration (A–C), molar ratio of crosslinking agents to HPAMAM (D–F), and crosslinking time (G–I) on resistance and weight gain rate of silver-coated fibers.

likely because of the crosslinked HPAMAM layer covering the fiber surface. Five new diffraction peaks in the silver-plated fibers appear at 2θ values of 38.27, 44.47, 64.58, 77.58, and 81.63°, which correspond to the (111), (200), (220), (311), and (222) planes of face-centered cubic silver,[42] respectively (JCPDS No.4-783). The characteristic peaks of PPTA are significantly weaker in the X-ray diffraction (XRD) of the silver-plated fibers. Therefore, the silver-plated fibers must be covered with a dense silver layer.

The thermal stability of the fibers was studied by thermogravimetric analysis using PPTA, ECH_1HP_{20}-PPTA, and ECH_1HP_{20}-PPTA/Ag as representative materials (Figure 5B). The weight loss of the pure PPTA fibers is about 56.58% in 500–600 °C, which is caused by the decomposition of the aramid backbone.[2] The modified fibers (ECH_1HP_{20}-PPTA) show about 4.51% weight loss in 0–100 °C as ECH_1HP_{20} can decompose at relatively low temperature, and the main chain of ECH_1HP_{20}-PPTA decomposes at >500 °C just like pristine PPTA. The silver-plated fibers (ECH_1HP_{20}-PPTA/Ag) has much less weight loss than both PPTA and ECH_1HP_{20}-PPTA, likely because of the high melting point of silver (~960 °C). When the heating temperature reaches 800 °C (i.e., at the end of the thermogravimetric experiment), the residual mass is 36.97, 47.90, and 71.46% for PPTA, ECH_1HP_{20}-PPTA, and ECH_1HP_{20}-PPTA/Ag, respectively. The results verify the existence of the silver layer and indicate that the synthetic procedures do not damage the thermal stability of the fibers.

Table 3 shows the tensile strength and the elongation at break of the fibers. The modification process hardly damages the mechanical properties of PPTA, as the three modified fibers have only about 2% less tensile strength compared with the pristine PPTA fibers. The three silver-plated fibers retain about 97% of tensile strength of PPTA, and the strength loss comes from the silver layer on the fiber surface rather than within the fibers. Interestingly, the tensile strength of the silver-plated fibers follows the same order of the electrical conductivity of the crosslinking agent used for HPAMAM (i.e., DGDE > ECH > EGDE), probably because an uneven silver layer tends to reduce strength more seriously. In sum, the fibers still possess excellent mechanical properties after silver plating.

https://doi.org/10.1021/acsomega.2c00143
ACS Omega 2022, 7, 17014–17023

3.2. Variables that Influence the Resistance of the Silver-Plated Fibers. Figure 6 A−C shows the changes of the resistance and weight gain rate of the three silver-plated conductive fibers with the concentration of HPAMAM. When the concentration of crosslinked HPAMAM is 20 g/L, the resistance of fibers is the lowest, reaching 0.110, 0.140, and 0.096 Ω/cm for ECH_1HP_{20}-PPTA, $EGDE_1HP_{20}$-PPTA, and $DGDE_1HP_{20}$-PPTA, respectively. When the crosslinked HPAMAM is less than 20 g/L, there is not enough silver adsorbed on the fibers, which reduces the conductivity of the final fibers. On the other hand, when the crosslinked HPAMAM is more than 20 g/L, the silver film on the fiber surface is thicker and attached less firmly, which results in an uneven silver layer and poor conductivity. The change of weight gain rate of the fibers has the exact opposite trend of resistance, which can be explained by the SEM findings. When the concentration of HPAMAM is less than 20 g/L, the weight gain rate increases as the silver layer on the fiber surface becomes denser, which improves conductivity. However, when the concentration of HPAMAM exceeds 20 g/L, the agglomerated shedding of silver particles decreases the weight gain rate and the electrical conductivity.

Figure 6D−F shows the changes of resistance and weight gain rate with the amount of the crosslinking agent when the concentration of HPAMAM is held constant at 20 g/L. In general, a higher amount of the crosslinking agent increases resistance and reduces conductivity. When only a small amount of the crosslinking agent is applied, the crosslinked HPAMAM forms a loose network structure that is beneficial to the chelation of Ag(I). Accordingly, the fibers adsorb more Ag(I), the deposition rate becomes higher, which increases the stability of the plating solution, and in turn increases the amount of Ag particles deposited. When there are excessive crosslinking agents, most of the amino groups will be crosslinked and the degree of crosslinking will be too high. Consequently, the adsorption of Ag(I) will be poorer, and the network structure will be tighter and too hydrophobic. To attain the best conductivity, Ag(I) should ideally enter the HPAMAM network and not be deposited on the PPTA fiber surface. The optimal molar ratio of HPAMAM to crosslinking agent is 1:2 for ECH and 1:1 for EGDE and DGDE. The difference is likely because the number of epoxy groups in the crosslinking reagent affects the degree of crosslinking, and ECH has only one epoxy group, whereas both EGDE and DGDE have two.

The influence of crosslinking time was evaluated by crosslinking 20 g/L HPAMAM with 1:2 ECH, 1:1 EGDE, and 1:1 DGDE, and the results are shown in Figure 6G−I. For ECH_2HP_{20}-PPTA/Ag, resistance is higher when the crosslinking time is less than 3 h, probably because a low degree of crosslinking reduces the chelating ability of the HPAMAM gel to adsorb Ag(I). Although the high weight gain rate suggests significant deposition of silver on the fibers, the HPAMAM film crosslinked by the small ECH molecule is uneven, thus causing high resistance. Resistance is also higher when the crosslinking time is longer than 3 h, it is also because a large number of amino groups are crosslinked, resulting in poor adsorption of Ag(I). At the same time, the network structure is too tighter and the hydrophilicity is poor due to a large degree of crosslinking. Low resistance and high silver content can be obtained with a short crosslinking time of 1 h for $EGDE_1HP_{20}$-PPTA/Ag, but 4 h is necessary for $DGDE_1HP_{20}$-PPTA/Ag, probably because DGDE has a lower crosslinking reactivity due to its long chain structure. The optimal resistance is 0.068, 0.140, and 0.067 Ω/cm for ECH_2HP_{20}-PPTA/Ag, $EGDE_1HP_{20}$-PPTA/Ag, and $DGDE_1HP_{20}$-PPTA/Ag adopting a crosslinking time of 3, 1, and 4 h, respectively.

The overall conductivity of the silver-coated fibers falls in the order of $DGDE_xHP_y$-PPTA/Ag > ECH_xHP_y-PPTA/Ag > $EGDE_xHP_y$-PPTA/Ag, likely because the crosslinked HPAMAM network structure formed by the long-chain DGDE is relatively loose, which helps the chelation of Ag(I) and creates a more uniform HPAMAM (and thus silver) layer. The conductive fibers prepared in the current work outperform many other reported conductive fibers prepared by electroless plating (Table 4). Therefore, modification with crosslinked HPAMAM is an effective pretreatment method for the electroless plating of aramid fibers.

Table 4. Comparison of Electrical Resistance of Different Conductive Fibers

conductive fibers	resistance (Ω/cm)	reference
silvered PPTA fibers prepared by the wet chemical method	1.000	43
silver-plated nylon fibers prepared by heat scanning	2.800	12
nickel-modified copper-plated PPTA fibers	0.351	44
NaH/DMSO-treated silver-plated PPTA fibers	0.210	45
silvered PPTA fibers modified by crosslinked chitosan	0.380	21
silver-plated PPTA fibers by employing low-temperature oxygen plasma treatment and dopamine functionalization	0.890	20
ECH_2HP_{20}-PPTA/Ag	0.068	this work
$EGDE_1HP_{20}$-PPTA/Ag	0.140	this work
$DGDE_1HP_{20}$-PPTA/Ag	0.067	this work

3.3. Firmness of Silver-Plated Fibers. The binding firmness of the silver-plated fibers was assessed by measuring the electrical resistance of the fibers after ultrasonic washing (Figure 7A). Ultrasonic treatment increases the resistance of $EGDE_1HP_{20}$-PPTA/Ag more rapidly than ECH_2HP_{20}-PPTA/Ag and $DGDE_1HP_{20}$-PPTA/Ag (Figure 7B), likely because the silver layer of $EGDE_1HP_{20}$-PPTA/Ag fibers does not have a uniform thickness and the silver particles fall off easily. Three ultrasonic washing cycles (10 min each) do not have a major impact on resistance, and the resistance of $DGDE_1HP_{20}$-PPTA/Ag increases from 0.067 to only 0.21 Ω/cm after 30 min. In addition, the resistance of $DGDE_1HP_{20}$-PPTA/Ag only increases to 0.45 Ω/cm when ultrasonic washing is increased to five 10 min cycles.

Conductive fibers also need to be flexible enough to maintain their properties upon deformation such as bending. The twisted $DGDE_1HP_{20}$-PPTA/Ag fibers close the circuit in Figure 7C without any problem and can light up the bulb successfully.

4. CONCLUSIONS

This paper provides a facile and efficient method to prepare silver-plated conductive PPTA fibers with excellent electrical conductivity and mechanical properties. Crude PPTA is first modified by crosslinked HPAMAM, and the final conductive fibers are prepared from the electroless silver plating of the modified PPTA. The crosslinked HPAMAM is essential to

https://doi.org/10.1021/acsomega.2c00143
ACS Omega 2022, 7, 17014−17023

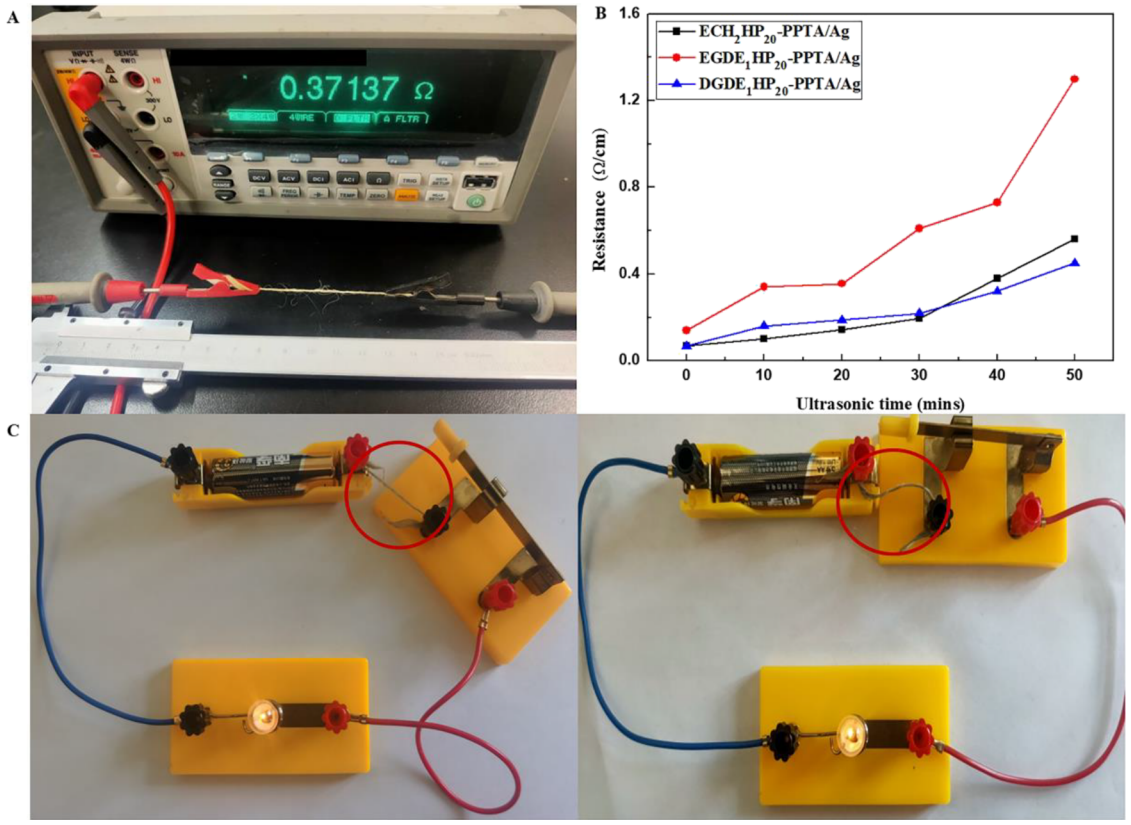

Figure 7. Photograph of resistance test equipment (A), variation of electrical resistance for silver-plated fibers with ultrasonic time (B), and photographs of the bulb powered through the conductive fibers subjected to bending (C).

creating the silver coating on the PPTA matrix. Three crosslinking agents were tested. The dosages of the crosslinking agent, the dosage of HPAMAM, and the time of crosslinking were all optimized to improve the performance of the conductive fibers. The $DGDE_1HP_{20}$-PPTA/Ag fibers attain the lowest resistance of 0.067 Ω/cm when the crosslinking time is 4 h, the HPAMAM concentration is 20 g/L, and the ratio of the crosslinking agent DGDE to HPAMAM is 1:1. The silver-plated fibers retain 97% of the tensile strength of the original PPTA fibers. The silver layer is more firmly attached to the PPTA matrix in $DGDE_1HP_{20}$-PPTA/Ag than in other fibers, and the resistance of $DGDE_1HP_{20}$-PPTA/Ag increases to only 0.45 Ω/cm after 5 ultrasonic cycles. The silver-plated PPTA fibers with high electrical conductivity and excellent mechanical properties are expected to see promising applications in various flexible conductive devices.

AUTHOR INFORMATION

Corresponding Authors

Rongjun Qu − *School of Chemistry and Materials Science, Ludong University, Yantai 264025, China; Yantai Research Institute for the Transformation of Old and New Kinetic Forces, Yantai 264025, China*; Email: rongjunqu@sohu.com, +86 535 6699201

Changmei Sun − *School of Chemistry and Materials Science, Ludong University, Yantai 264025, China; Yantai Research Institute for the Transformation of Old and New Kinetic Forces, Yantai 264025, China*; Email: sunchangmei0535@126.com

Authors

Xue Geng − *School of Chemistry and Materials Science, Ludong University, Yantai 264025, China; Yantai Research Institute for the Transformation of Old and New Kinetic Forces, Yantai 264025, China*; orcid.org/0000-0002-4513-5596

Xiangyu Kong − *School of Chemistry and Materials Science, Ludong University, Yantai 264025, China; Yantai Research Institute for the Transformation of Old and New Kinetic Forces, Yantai 264025, China*

Shengnan Geng − *School of Chemistry and Materials Science, Ludong University, Yantai 264025, China; Yantai Research Institute for the Transformation of Old and New Kinetic Forces, Yantai 264025, China*

Jiafei Wang − *School of Chemistry and Materials Science, Ludong University, Yantai 264025, China; Yantai Research Institute for the Transformation of Old and New Kinetic Forces, Yantai 264025, China*

Ying Zhang − *School of Chemistry and Materials Science, Ludong University, Yantai 264025, China; Yantai Research Institute for the Transformation of Old and New Kinetic Forces, Yantai 264025, China*

Chunnuan Ji − *School of Chemistry and Materials Science, Ludong University, Yantai 264025, China; Yantai Research Institute for the Transformation of Old and New Kinetic Forces, Yantai 264025, China*

Complete contact information is available at: https://pubs.acs.org/10.1021/acsomega.2c00143

https://doi.org/10.1021/acsomega.2c00143
ACS Omega 2022, 7, 17014−17023

Author Contributions

X.G.: Investigation, formal analysis, and writing-original draft preparation; X.K.: writing-review and editing and software; S.G.: Investigation and validation; R.Q.: Conceptualization, methodology, funding acquisition, and project administration; J.W.: Investigation and software; Y.Z.: Writing-review and editing, validation, and resources; C.S.: Conceptualization and methodology; C.J.: Software and data curation.

Notes

The authors declare no competing financial interest.

■ ACKNOWLEDGMENTS

The authors are grateful for the financial support by the National Natural Science Foundation of China (52073135, 51673089, and 51903114); Yantai Research Institute for the Transformation of Old and New Kinetic Forces (2019XJDN001); and Natural Science Foundation of Shandong Province (ZR2020ME066).

■ REFERENCES

(1) Huang, S.; Wang, J.; Li, Y.; Tang, J.; Zhang, X. Microstructure characterization and formation mechanism of colloid palladium for activation treatment on the surface of PPTA fibers. *Appl. Surf. Sci.* **2020**, *516*, No. 146134.

(2) Zhang, Y.; Qu, R.; Wang, Y.; Jia, X.; Sun, C.; Sun, H.; Ji, C.; Zhang, Y.; Zhu, Q. Enhancement of para-aramid fibers by depositing poly-p-paraphenylene terephthalamide oligomer modified multi-walled carbon nanotubes. *Result Mater.* **2021**, *9*, No. 100170.

(3) Zhang, Z.; Zhao, Y.; Li, H.; Percec, S.; Yin, J.; Ren, F. Nanoparticle-Infused UHMWPE Layer as Multifunctional Coating for High-Performance PPTA Single Fibers. *Sci. Rep.* **2019**, *9*, 7183.

(4) Tamargo-Martínez, K.; Montes-Morán, M. A.; Martínez-Alonso, A.; Tascón, J. M. D. Effect of non-oxidative plasma treatments on the surface properties of poly(p-phenylene terephthalamide) (PPTA) and poly(p-phenylene benzobisoxazole) (PBO) fibres as measured by inverse gas chromatography. *J. Chromatogr. A* **2020**, *1634*, No. 461655.

(5) Yilmaz, D. E.; van Duin, A. C. T. Investigating structure property relations of poly (p-phenylene terephthalamide) fibers via reactive molecular dynamics simulations. *Polymer* **2018**, *154*, 172−181.

(6) Liu, Z.; Li, L.; Zhao, Z.; Liu, Y.; Lu, M. Antistatic silk fabric through sericin swelling-fixing treatment with aminated carbon nanotubes. *Mater. Sci. Eng., B* **2017**, *226*, 72−77.

(7) Gu, S.; Liu, H.; Li, X.; Mercier, C.; Li, Y. Interfacial designing of PP/GF composites by binary incorporation of MAH-g-PP and lithium bis(trifloromethanesulfonyl)imide: Towards high strength composites with excellent antistatic performance. *Compos. Sci. Technol.* **2018**, *156*, 247−253.

(8) Bhardwaj, P.; Grace, A. N. Antistatic and microwave shielding performance of polythiophene-graphene grafted 3-dimensional carbon fibre composite. *Diamond Relat. Mater.* **2020**, *106*, No. 107871.

(9) Gürakın, H. K.; Turan, A. C.; Deligöz, H. Synthesis of a novel polyester-ether copolymer and its derivatives as antistatic additives for thermoplastic films. *Polym. Test.* **2020**, *81*, No. 106214.

(10) Tan, Y.; Li, J.; Gao, Y.; Li, J.; Guo, S.; Wang, M. A facile approach to fabricating silver-coated cotton fiber non-woven fabrics for ultrahigh electromagnetic interference shielding. *Appl. Surf. Sci.* **2018**, *458*, 236−244.

(11) Zhou, Y.; Sun, Z.; Jiang, L.; Chen, S.; Ma, J.; Zhou, F. Flexible and conductive meta-aramid fiber paper with high thermal and chemical stability for electromagnetic interference shielding. *Appl. Surf. Sci.* **2020**, *533*, No. 147431.

(12) Jang, J.; Zhou, H.; Lee, J.; Kim, H.; In, J. B. Heat Scanning for the Fabrication of Conductive Fibers. *Polymers* **2021**, *13*, 1405.

(13) Wang, A.; Zhang, X.; Chen, F.; Fu, Q. Aramid nanofiber framework supporting graphene nanoplate via wet-spinning for a high-performance filament. *Carbon* **2021**, *179*, 655−665.

(14) Miao, Y.; Chen, H.; Cui, G.; Qi, Y. Preparation of new conductive organic coating for the fiber reinforced polymer composite oil pipe. *Surf. Coat. Technol.* **2021**, *412*, No. 127017.

(15) Ting Gu; Zhu, D.; Lu, S. Surface Functionalization of Silver-Coated Aramid Fiber. *Polym. Sci. Ser. A Chem. Phys.* **2020**, *62*, 196−204.

(16) Han, W.; Qian, X.; Ma, H.; Wang, X.; Zhang, Y. Effect of nickel electroplating followed by a further copper electroplating on the micro-structure and mechanical properties of high modulus carbon fibers. *Mater. Today Commun.* **2021**, *27*, No. 102345.

(17) Wang, Q.; Xiao, S.; Shi, S. Q.; Xu, S.; Cai, L. Self-bonded natural fiber product with high hydrophobic and EMI shielding performance via magnetron sputtering Cu film. *Appl. Surf. Sci.* **2019**, *475*, 947−952.

(18) Tang, J.; Zhang, X.; Wang, J.; Zou, R.; Wang, L. Achieving flexible and durable electromagnetic interference shielding fabric through lightweight and mechanically strong aramid fiber wrapped in highly conductive multilayer metal. *Appl. Surf. Sci.* **2021**, *565*, No. 150577.

(19) Wang, W.; Li, W.; Gao, C.; Tian, W.; Sun, B.; Yu, D. A novel preparation of silver-plated polyacrylonitrile fibers functionalized with antibacterial and electromagnetic shielding properties. *Appl. Surf. Sci.* **2015**, *342*, 120−126.

(20) Sun, Z.; Zhou, Y.; Li, W.; Chen, S.; You, S.; Ma, J. Preparation of Silver-Plated Para-Aramid Fiber by Employing Low-Temperature Oxygen Plasma Treatment and Dopamine Functionalization. *Coatings* **2019**, *9*, 599.

(21) Yu, D.; Mu, S.; Liu, L.; Wang, W. Preparation of electroless silver plating on aramid fiber with good conductivity and adhesion strength. *Colloids Surf., A* **2015**, *483*, 53−59.

(22) Tang, J.; Wang, J.; Zhang, X.; Tian, Z. Multiscale analysis of enclosed nickel metal layer constructed via a palladium-triggered autocatalytic reaction on aramid fiber surfaces. *Surf. Coat. Technol.* **2021**, *405*, No. 126706.

(23) Liang, J.; Zou, X.; Shao, Q.; Sun, J.; Tang, Z. Preparation and properties of conductive silver-plated aramid fibers. *J. Funct. Mater.* **2012**, *43*, 2757−2762.

(24) Wang, W.; Li, R.; Tian, M.; Liu, L.; Zou, H.; Zhao, X.; Zhang, L. Surface silverized meta-aramid fibers prepared by bio-inspired poly(dopamine) functionalization. *ACS Appl. Mater. Interfaces* **2013**, *5*, 2062−2069.

(25) Saadati, A.; Hasanzadeh, M.; Seidi, F. Biomedical application of hyperbranched polymers: Recent Advances and challenges. *TrAC, Trends Anal. Chem.* **2021**, *142*, No. 116308.

(26) Sohail, I.; Bhatti, I. A.; Ashar, A.; Sarim, F. M.; Mohsin, M.; Naveed, R.; Yasir, M.; Iqbal, M.; Nazir, A. Polyamidoamine (PAMAM) dendrimers synthesis, characterization and adsorptive removal of nickel ions from aqueous solution. *J. Mater. Res. Technol.* **2020**, *9*, 498−506.

(27) Yin, R.; Niu, Y.; Zhang, B.; Chen, H.; Yang, Z.; Yang, L.; Cu, Y. Removal of Cr(III) from aqueous solution by silica-gel/PAMAM dendrimer hybrid materials. *Environ. Sci. Pollut. R.* **2019**, *26*, 18098−18112.

(28) Ren, B.; Wang, K.; Zhang, B.; Li, H.; Niu, Y.; Chen, H.; Yang, Z.; Li, X.; Zhang, H. Adsorption behavior of PAMAM dendrimers functionalized silica for Cd(II) from aqueous solution: Experimental and theoretical calculation. *J. Taiwan Inst. Chem. Eng.* **2019**, *101*, 80−91.

(29) Karakhanov, E. A.; Maximov, A. L.; Zakharyan, E. M.; Zolotukhina, A. V.; Ivanov, A. O. Palladium nanoparticles on dendrimer-containing supports as catalysts for hydrogenation of unsaturated hydrocarbons. *Mol. Catal.* **2017**, *440*, 107−119.

(30) Zhu, Y.; Niu, Y.; Li, H.; Ren, B.; Qu, R.; Chen, H.; Zhang, Y. Removal of Cd(II) and Fe(III) from DMSO by silica gel supported PAMAM dendrimers: Equilibrium, thermodynamics, kinetics and mechanism. *Ecotoxicol. Environ. Safety* **2018**, *162*, 253−260.

(31) Farmanzadeh, D.; Ghaderi, M. A computational study of PAMAM dendrimer interaction with trans isomer of picoplatin anticancer drug. *J. Mol. Graphics Modell.* **2018**, *80*, 1−6.

https://doi.org/10.1021/acsomega.2c00143
ACS Omega 2022, 7, 17014−17023

(32) Lin, H.; Han, S.; Dong, Y.; Ling, W.; He, Y. Structural Characteristics and Functional Properties of Corncob Modified by Hyperbranched Polyamide for the Adsorption of Cr (VI). *Water, Air, Soil Pollut.* **2018**, *229*, 117.
(33) Li, J.; Zhu, W.; Zhang, S.; Gao, Q.; Li, J.; Zhang, W. Amine-terminated hyperbranched polyamide covalent functionalized graphene oxide-reinforced epoxy nanocomposites with enhanced toughness and mechanical properties. *Polym. Test.* **2019**, *76*, 232−244.
(34) Wei, C.; Cheng, J.; Chen, P.; Wei, B.; Gao, D.; Xu, D. Facile electroless copper plating on diamond particles without conventional sensitization and activation. *Adv. Powder Technol.* **2019**, *30*, 2751−2758.
(35) Yang, X.; Tu, Q.; Shen, X.; Zhu, P.; Li, Y.; Zhang, S. A Novel Method for Deposition of Multi-Walled Carbon Nanotubes onto Poly(p-Phenylene Terephthalamide) Fibers to Enhance Interfacial Adhesion with Rubber Matrix. *Polymers* **2019**, *11*, 374.
(36) Yu, F.; Teng, C.; Qin, M.; Liu, B.; Zhang, K.; Ni, J.; Yu, M. Performance of Silver-deposited Aramid Fibers. *Chinese J. Mater. Res.* **2017**, *31*, 585−590.
(37) Zhang, Y.; Qu, R.; Xu, T.; Zhang, Y.; Sun, C.; Ji, C.; Wang, Y. Fabrication of Triethylenetetramine Terminal Hyperbranched Dendrimer-Like Polymer Modified Silica Gel and Its Prominent Recovery Toward Au (III). *Front. Chem.* **2019**, *7*, 577.
(38) Jawad, A. H.; Mamat, N. F. H.; Hameed, B. H.; Ismail, K. Biofilm of cross-linked Chitosan-Ethylene Glycol Diglycidyl Ether for removal of Reactive Red 120 and Methyl Orange: Adsorption and mechanism studies. *J. Environ. Chem. Eng.* **2019**, *7*, No. 102965.
(39) Wang, Y.; Qu, R.; Pan, F.; Jia, X.; Sun, C.; Ji, C.; Zhang, Y.; An, K.; Mu, Y. Preparation and characterization of thiol- and amino-functionalized polysilsesquioxane coated poly(p -phenylenetherephthal amide) fibers and their adsorption properties towards Hg(II). *Chem. Eng. J.* **2017**, *317*, 187−203.
(40) Li, Q.; Xu, B.; Zhuang, L.; Xu, X.; Wang, G.; Zhang, X.; Chen, J.; Tang, Y. Preparation, characterization, adsorption kinetics and thermodynamics of chitosan adsorbent grafted with a hyperbranched polymer designed for Cr(VI) removal. *Cellulose* **2018**, *25*, 3471−3486.
(41) Khodayari, A.; Sohrabnezhad, S. Fabrication of MIL-53(Al)/Ag/AgCl plasmonic nanocomposite: An improved metal organic framework based photocatalyst for degradation of some organic pollutants. *J. Solid State Chem.* **2021**, *297*, No. 122087.
(42) Wang, K.; Huang, Z.; Jin, X.; Zhang, D.; Wang, J. MOF−derived hollow porous ZnFe2O4/AgCl/Ag/C nanotubes with magnetic−dielectric synergy as high−performance photocatalysts for hydrogen evolution reaction. *Chem. Eng. J.* **2021**, *422*, No. 130140.
(43) Onggar, T.; Amrhein, G.; Abdkader, A.; Hund, R.; Cherif, C. Wet-chemical method for the metallization of a para-aramid filament yarn wound on a cylindrical dyeing package. *Text. Res. J.* **2017**, *87*, 1192−1202.
(44) Zhang, H.; Zou, X.; Sun, J. Influence of polyethylene glycol 6000 and potassium ferrocyanide on electroless copper plating at the nickel-modified surface of para-aramid fibers. *J. Compos. Mater.* **2012**, *46*, 3001−3009.
(45) Zhang, H.; Zou, X.; Liang, J.; Ma, X.; Tang, Z.; Sun, J. Development of electroless silver plating on Para-aramid fibers and growth morphology of silver deposits. *J. Appl. Polym. Sci.* **2012**, *124*, 3363−3371.

https://doi.org/10.1021/acsomega.2c00143
ACS Omega 2022, 7, 17014−17023